# Motor System Interactions in the Beta Band Decrease during Loss of Consciousness

Nicole C. Swann[1], Coralie de Hemptinne[1], Ryan B. Maher[2], Catherine A. Stapleton[3], Lingzhong Meng[1], Adrian W. Gelb[1], and Philip A. Starr[1]



## Abstract

■ Communication between brain areas and how they are influenced by changes in consciousness are not fully understood. One hypothesis is that brain areas communicate via oscillatory processes, utilizing network-specific frequency bands, that can be measured with metrics that reflect between-region interactions, such as coherence and phase amplitude coupling (PAC). To evaluate this hypothesis and understand how these interactions are modulated by state changes, we analyzed electrophysiological recordings in humans at different nodes of one well-studied brain network: the basal ganglia–thalamocortical loops of the motor system during loss of consciousness induced by anesthesia. We recorded simultaneous electrocorticography over primary motor cortex (M1) with local field potentials from subcortical motor regions (either basal ganglia or thalamus) in 15 movement disorder patients during anesthesia (propofol) induction as a part of their surgery for deep brain stimulation. We observed reduced coherence and PAC between M1 and the subcortical nuclei, which was specific to the beta band (~18–24 Hz). The fact that this pattern occurs selectively in beta underscores the importance of this frequency band in the motor system and supports the idea that oscillatory interactions at specific frequencies are related to the capacity for normal brain function and behavior. ■

## INTRODUCTION

How do functionally related brain areas communicate over long distances? One hypothesis is based on oscillatory synchronization in specific frequency bands, usually lower than ~50 Hz (Siegel, Donner, & Engel, 2012). Coherence is a simple measure of oscillatory synchronization that may support long-distance neural interactions. It reflects interactions between brain areas related to the consistency of the phases and amplitudes of their neuronal signals (Fries, 2005). On the other hand, higher-frequency, broadband activity ("broadband gamma", 70–250 Hz) seems to reflect local neural activity (Manning, Jacobs, Fried, & Kahana, 2009; Miller et al., 2007). Canolty and colleagues demonstrated that, in some instances, broadband gamma amplitude is modulated by the phase of lower-frequency oscillatory rhythms (Canolty et al., 2006). This phase amplitude coupling (PAC) provides a mechanism that could explain how low-frequency oscillatory changes, which are well suited to coordinate activity over long distances, can influence local neuronal activity (Canolty & Knight, 2010; Fries, 2005). When PAC is calculated from the phase and amplitude of signals recorded from two different brain areas, it may also reflect interactions between brain regions.

Transitions in consciousness afford an opportunity to evaluate how these basic measurements of brain interactions change in the context of profound behavior/state changes. Although the underlying causal mechanisms of consciousness remain unclear, there is converging evidence that transitions of consciousness are characterized by a change of network dynamics wherein local brain networks become more isolated from one another, disrupting the brain's ability to integrate information (Lewis et al., 2012; Alkire, Hudetz, & Tononi, 2008). Because all but the most basic forms of behavior are only possible in the conscious state, we hypothesized that the most functionally important network interactions are only present in the conscious state. To better understand how those interactions might mediate behavior and, perhaps, relate to communication in brain networks, we sought to study how simple metrics of brain interactions (coherence and PAC) in the motor system change during anesthesia-induced transitions in consciousness.

To address this goal, we combined electrocorticography (ECoG) and subcortical local field potential (LFP) recordings in movement disorder patients undergoing surgical implantation of deep brain stimulation (DBS) leads (de Hemptinne et al., 2013, 2015). This approach provides a unique opportunity to acquire field potential data from functionally related cortical and subcortical structures (primary motor cortex [M1] and motor territories of the basal ganglia and thalamus). Because DBS targets vary across individuals/diagnoses, we have

[1]University of California San Francisco, [2]Fidere Anesthesia Consultants, Mountain View, CA, [3]Alta Bates Summit Medical Center, Berkeley, CA



Journal of Cognitive Neuroscience 28:1, pp. 84–95
doi:10.1162/jocn_a_00884

the opportunity to sample from a number of different subcortical nodes in the basal ganglia–thalamocortical (BGTC) loop (although this does increase variability in our sample). The BGTC circuit is particularly well suited to address questions concerning network interactions, because structural connectivity in the motor loop is relatively well defined, with connections from cortex to basal ganglia to thalamus and then back to cortex (Alexander, DeLong, & Strick, 1986). Additionally, the electrophysiological signatures in the motor system have been studied extensively. The beta frequency range (13–30 Hz) dominates and is dynamically modulated during movement (Brovelli et al., 2004; Kuhn et al., 2004; Cassidy et al., 2002; Crone, Miglioretti, Gordon, Sieracki, et al., 1998; Sanes & Donoghue, 1993; Murthy & Fetz, 1992; Pfurtscheller, 1981). We hypothesized that loss of consciousness would be characterized by reduced interactions between cortical and subcortical regions, measured with coherence and inter-region PAC, and that this would be particularly prominent in the beta frequency band.

## METHODS

### Patients

Fifteen patients (4 women/11 men, average age = 62 years) were recruited from the Surgical Movement Disorders Clinic at the University of California, San Francisco. Patients were scheduled to undergo surgery to implant a permanent subcortical DBS lead to treat their movement disorders. All patients were simultaneously participating in a study of the contribution of cortical oscillatory activity to movement disorders pathophysiology, using ECoG from a subdural strip array inserted through the standard frontal burr hole used for DBS insertion, and temporarily placed over the primary motor cortex (de Hemptinne et al., 2013; Shimamoto et al., 2013; Crowell et al., 2012). Our standard surgical procedure requires that patients be awake for microelectrode mapping and DBS lead insertion, followed by anesthesia induction (for wound closure). This procedure provides the opportunity for brain recording during anesthesia-induced loss of consciousness, avoiding the need to administer anesthetics solely for research purposes.

The goal of this study was to examine interactions between nodes of the motor system during loss of consciousness, rather than focusing on a specific movement disorder. Therefore, we included patients with varying diagnoses and varying subcortical targets within the motor network to enable the identification of network motifs common to changes in consciousness independent of disease state. Twelve of the patients had Parkinson disease (PD), two had essential tremor (ET), and one had primary dystonia. Four PD patients had DBS leads placed into the globus pallidus interna (GPi), whereas the other eight had subthalamic nucleus (STN) leads, with target choice dictated by clinical criteria (Follett et al., 2010). The DBS target for ET patients was the ventrolateral thalamus. The target for the dystonia patient was GPi. The study methodologies were approved by the institutional ethics committee and are in agreement with the Declaration of Helsinki. All patients provided written informed consent to participate in the study, and the use of a temporary cortical ECoG array placed for research purposes was an explicit part of the consent discussion.

### ECoG Strip Placement

ECoG was recorded from one hemisphere during the surgery. For patients receiving unilateral DBS, the ECoG was placed ipsilateral to the side of the DBS. For patients receiving bilateral surgery, the side of the ECoG was determined based on the clearest anatomic demarcation of the central sulcus on preoperative MRI. Eleven patients had left side recordings, whereas four had right.

The data from the dystonia patient and five PD patients were collected with a six-electrode ECoG strip (1 cm spacing between electrodes; see Figure 1A), and the other seven PD patients and both ET patients were recorded with a 28-electrode ECoG strip (4 mm spacing between electrodes; see Figure 1B). The type of ECoG strip used depended on the parent study of movement disorders physiology, because during this study period, we transitioned from the lower spatial resolution recording to a higher-resolution technique. Each strip was placed with at least one electrode covering M1. The intended target location for the center of the ECoG strip was the arm area of M1, 3 cm from the midline and slightly medial to the hand knob (Yousry et al., 1997). Adequate localization of the ECoG strip was confirmed using either preoperative MRI merged to an intraoperative CT (13 participants) or using intraoperative lateral fluoroscopy with a radio-opaque

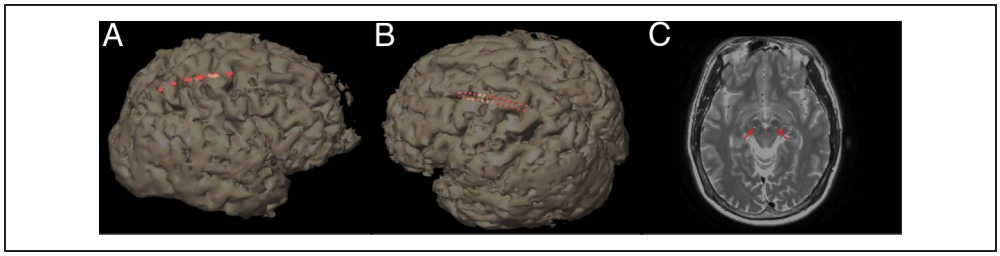


**Figure 1.** 3D brain reconstructions of each participant's MRI with the low-resolution (A) and high-resolution (B) ECoG strips and the subcortical DBS electrode, positioned in STN (indicated with red arrows) (C). Electrode locations (shown in red) are visualized by merging an intraoperative CT with a preoperative MRI.

marker placed on the skin indicating the intended target in M1 that was visible relative to the electrode strip (2 participants), as previously described (de Hemptinne et al., 2013, 2015; Shimamoto et al., 2013; Crowell et al., 2012). In all participants, functional localization was also examined using somatosensory evoked potentials (SSEPs, frequency = 2 Hz, pulse width = 200 μs, pulse train length = 160, amplitude = 25–40 mAmp), as has been reported (de Hemptinne et al., 2013; Shimamoto et al., 2013; Crowell et al., 2012). Note that for the 28-electrode strip, there were two rows of 14 electrodes (see Figure 1B), so it was expected that two electrodes localized immediately anterior to the central sulcus would show a phase reversal relative to the postcentral sulcus electrodes.

### DBS Electrode Implantation

Anatomic targeting of the desired subcortical structure was performed as previously described (Starr et al., 2002, 2006; Papavassiliou et al., 2004). For the GPi and STN targets, the proper location was verified by eliciting movement-related single-cell discharge patterns (Starr et al., 2002). For all regions, the correct placement was verified by test stimulation, as well as intraoperative fluoroscopy (all patients), intraoperative CT (13 patients; Shahlaie, Larson, & Starr, 2011), and postoperative MRI (all patients).

### Consciousness Assessment and Anesthesia Parameters

Continuous recordings were taken after DBS placement, but prior to burr hole closure and DBS pulse generator placement, while the patients were slowly anesthetized with propofol. Data from PD patients were recorded after at least 12 hr off antiparkinsonian medications. Consciousness was assessed every 3 min using the Modified Observers Assessment of Alertness/Sedation Scale (MOAA/S; see Table 1; Chernik et al., 1990). Ratings were recorded by an anesthesiologist (AG, LM). When the clock started for the assessment session (time zero), a button was pressed, which generated a voltage deflection in an auxiliary channel digitized with the electrophysiology data. This synchronized the times noted by the anesthesiologist with the electrophysiology data.

Anesthesia induction with propofol was performed slowly with the goal of achieving an estimated plasma level (Marsh Model) of 4 mcg/ml at approximately 15 min (Smith et al., 1994). Induction ended when all patients no longer responded to painful stimulation according to MOAA/S scale (see Table 1). Propofol sedation had also been used during the drilling of the burr holes prior to intracranial recording but was stopped for subcortical mapping and DBS lead testing, at least 60 min prior to initiating the recordings analyzed here. This is ample time for the effects of propofol to wear off (Raz, Eimerl, Zaidel, Bergman, & Israel, 2010; Fechner et al., 2004).

**Table 1.** MOAA/S Responsiveness Scale

| *State* | *Responsiveness* |
|---|---|
| 5 | Responds readily to name spoken in normal tone |
| 4 | Lethargic response to name spoken in normal tone |
| 3 | Responds only after name is called loudly and/or repeatedly |
| 2 | Responds only after mild prodding or shaking |
| 1 | Responds only after painful trapezius squeeze |
| 0 | No response after painful trapezius squeeze |

Rating criteria for each state.

### ECoG and LFP Recordings

ECoG recordings were performed using either the Alpha Omega Microguide Pro, Alpha Omega, Inc. (Alpharetta, GA; for the six-electrode strip; Figure 1A) or the Tucker Davis Technologies Recording System (for the 28 electrode strip; Figure 1B). For the Alpha Omega system, data were sampled at 3000 Hz. Data from each of the five more posterior electrodes were referenced to the most anterior electrode. A needle electrode in the scalp served as the ground. Data were band-pass filtered at 1–500 Hz. For the Tucker Davis System, data were sampled at 3051 Hz. All electrodes were referenced to a scalp needle electrode that also served as the ground. Data were low-pass filtered at 1500 Hz. Because there was no high-pass filter applied during data acquisition, the mean of each electrode was subtracted during offline preprocessing to detrend the data. See Figure 2A for an example of the raw ECoG data.

LFP recordings were from the subcortical target ipsilateral to ECoG placement were recorded in a bipolar configuration from the middle two cylindrical contacts (1.5 mm height, 1.2 mm diameter) of a quadripolar lead (Medtronic model 3389, 0.5 mm between contacts, eight patients or Medtronic model 3387, 1.5 mm between contacts, seven patients), with Electrode 1 as the active and Electrode 2 as the reference. The guide tube for the DBS lead served as ground. For the six patients for whom the six-electrode cortical strip was used, the LFP recordings were done with the Alpha Omega system using the same Alpha Omega parameters described above for ECoG. For all the PD patients who were tested with the 28-electrode strip, LFP data were still collected using the hardware from the Alpha Omega system (which was necessarily present as it is FDA-approved for clinical microelectrode recordings for mapping); however, the analog signal was streamed to the Tucker Davis system and digitized there at 25,000 Hz sampling rate and then subsequently downsampled. For the sessions with ET patients, the Alpha Omega system was not present in the room, as microelectrode recordings were not used for ET. Thus, LFPs were recorded in the same manner as the ECoG electrodes (data

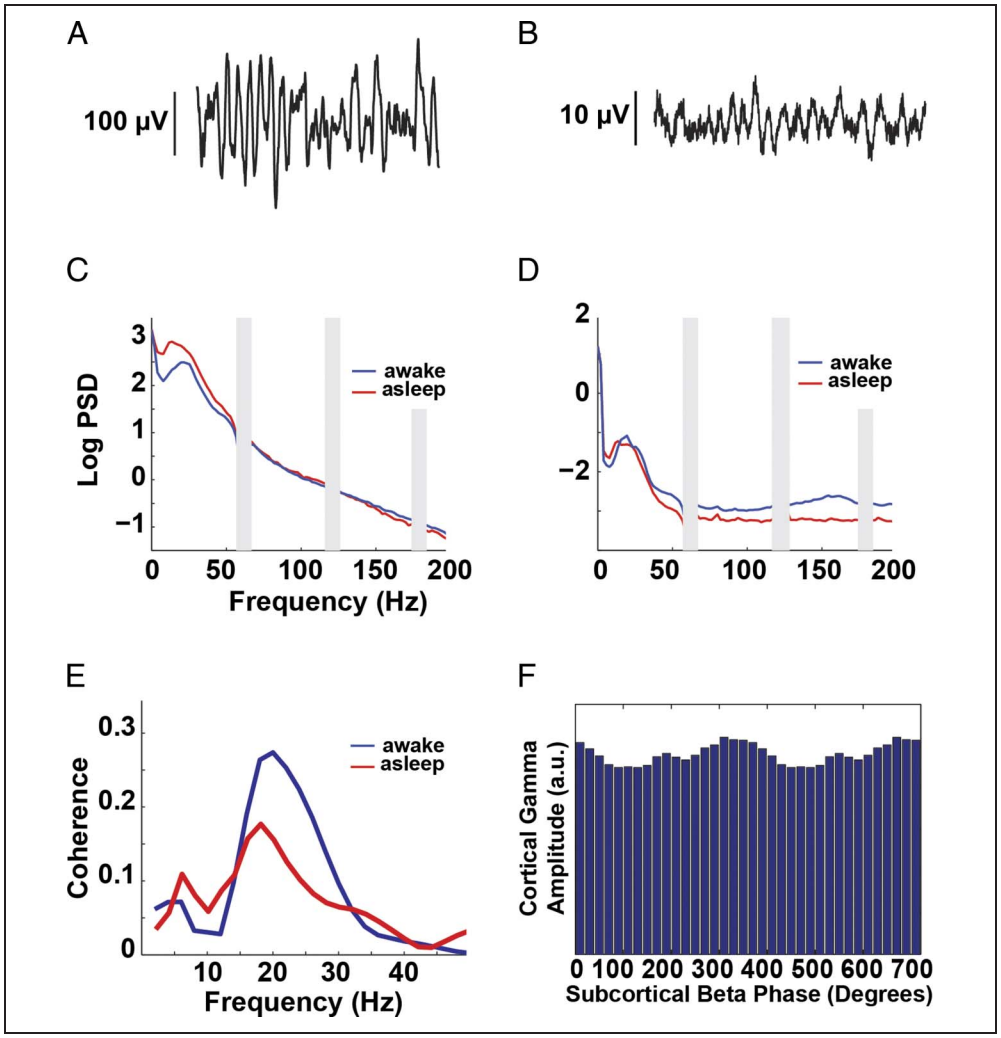


**Figure 2.** Example data from individual participant 6. One second of raw M1 ECoG (A) data and raw LFP data (from STN) (B). Log PSD from M1 (C) and STN (D). The gray bars indicate 60-Hz noise and the harmonics. (E) Coherence between M1 and STN. (F) Histogram of mean M1 broadband gamma amplitude (70–150 Hz) binned by subcortical beta phase (18–20 Hz). Here, modulation is apparent. A flat distribution would suggest no PAC.

from Electrodes 1 and 2 of the DBS electrode were both recorded with the needle electrode as the reference and ground) and then subsequently referenced in a bipolar configuration offline. See Figure 2B for an example of the raw LFP data.

### Electrophysiological Preprocessing

All data were initially down-sampled to 1000 Hz, and line frequency noise (at 60 Hz, 120 Hz, and 180 Hz) was removed using a third-order Butterworth notch filter, which spanned a 4-Hz range centered at each frequency (i.e., 58–62 Hz for 60 Hz). Data were then re-referenced. For the six-electrode strip, a bipolar montage was used such that each electrode was referenced to the anterior electrode (C1–C2, C2–C3, etc.). For the 28-electrode strip a common average reference was used including all ECoG electrodes (excluding any with obvious, continuous noise). Each reference strategy is best suited for the given electrode configuration: An average reference montage is not appropriate when there are only five active electrodes to contribute to the reference, and a bipolar reference is less optimal for the 28 electrode strip with small contacts and very close spacing. To determine if the different referencing schemes influenced our results, we re-ran our analyses using an average reference scheme for all participants, and the results were similar; thus, this difference in analysis is unlikely to have strongly influenced our findings. Subcortical LFP electrodes were processed in the same way as above (down-sampled and filtered). All raw data were manually inspected and periods of artifact (e.g., electrical artifact caused by medical equipment or movement) were noted and excluded from analysis.

During data recording, the anesthesiologist performed ratings every 3 min to assess the patient's level of consciousness (see Table 1). Data were assigned a consciousness rating according to the assessment at the end of each 3-min time segment. For instance, if after 3 min the anesthesiologist rated the patient's alertness as a 5 and at 6 min rated it as a 4, the segment of the electrophysiology data corresponding to 0–3 min would be marked as "State 5" and times 3–6 min would be marked as "State 4." Not all patients were observed at each state.

The longest artifact-free period of each state was used for analysis. On average, this was 218.1 sec and was always greater than 31 sec. Because both coherence and PAC can vary over time even without an overt change in behavioral state, we included the longest data segments possible for each participant and each level of consciousness. However, because coherence and PAC values can also be influenced by differences in the length of data analyzed, we conducted a control analysis to verify that differences in data length were not systematically driving our observed differences. In this analysis, for each participant, data of the same length from each state were used for comparison.

For each patient, the cortical electrode(s) that most closely corresponded to M1 were selected based on both the anatomical localization and SSEP waveforms. This was done prior to examining the data from the anesthesia induction file. For the 28-electrode strip, there were two rows of 14 electrodes, so we selected one M1 electrode from each row that met these same criteria. In this case, power, coherence, and PAC (described below) were calculated separately for each of these electrodes and then averaged for each electrode pair. For the six-electrode strip, the electrode selection procedure described above typically led to the selection of one electrode, which clearly lay over M1 (at the border of the central sulcus and the precentral gyrus), that also showed a clear SSEP phase reversal. For the 28-electrode strip, where the electrodes were smaller and spaced closer together, definitive selection of the two optimal M1 electrodes was less clear (regardless of reference scheme used). To test whether ambiguous selection of the M1 electrode may have influenced our results, we conducted a test wherein all electrodes on each strip were included in the analysis. (In this case, signal processing calculations described below were calculated for each electrode separately, and then the final results were averaged, such that each participant contributed only one data point to the group statistics.) Although this method clearly provides less spatial specificity, results were similar even when all electrodes were included. Thus, ambiguity in the selection of the optimal M1 electrode did not distort our results. The fact that results were similar for the M1 electrode, and the entire strip, most likely reflects the fact that the strip was placed to span precentral and postcentral gyri, which generate similar oscillatory signatures (Crone, Miglioretti, Gordon, Sieracki, et al., 1998).

### Electrophysiological Signal Processing

All analyses used a combination of custom Matlab scripts and EEGLAB functions (Delorme & Makeig, 2004). We implemented two main types of analyses. First, we analyzed the activity of each area (M1 and the subcortical region) separately. We calculated power spectral density (PSD) and PAC (Tort et al., 2008; Canolty et al., 2006) within each region. Analyses for each patient, state, and region (M1 and subcortical) were calculated separately in Matlab.

PSD analysis used the Welch method (*pwelch* function in Matlab with a 512-msec window, 256 msec of overlap; see Figure 2C and D for an example of PSD in one participant). Statistics were then calculated based on the log PSD values. However, results were similar if non-log-transformed values were used.

PAC was calculated using the Kullback–Leibler-based modulation index method, which has been previously described (de Hemptinne et al., 2013; Tort et al., 2008). In brief, the M1 ECoG and subcortical LFP signal were filtered separately using a two-way FIR1 filter (eegfilt with 'fir1' parameters). Low-frequency signals were filtered individually at frequencies ranging from 2 to 50 Hz, with a 2-Hz bandwidth, and the phase was extracted from this signal using a Hilbert transform. Similarly, the amplitude of the high-frequency broadband gamma signal was extracted by taking the Hilbert transform of the band-pass filtered data (70–150 Hz). Then the distribution of the instantaneous amplitude envelope was computed for every 20° interval of the instantaneous phase (see Figure 2F). The coupling (modulation index) between the phase of each low-frequency rhythm and the high-frequency amplitude was then determined by computing the entropy values of this distribution and normalizing by the maximum entropy value (Tort et al., 2008).

Second, we analyzed subcortical–cortical interactions by calculating coherence and cross-structure PAC. Analyses were performed for each participant and state separately, using signals from both the M1 ECoG and the subcortical LFP. We calculated coherence for frequencies ranging from 2 to 50 Hz, with a 2-Hz bandwidth, by filtering both the M1 ECoG and subcortical LFP using the same two-way FIR1 filter used to calculate PAC. Complex signals were then obtained for each filtered signal by taking the Hilbert transform. Coherence between the ECoG electrode(s) and the subcortical LFP was calculated using the corresponding autospectra ($W_{xx}$ and $W_{yy}$) and cross-spectra ($W_{xy}$) of the filtered complex signals.

$$\mathrm{Coh}(f) = \frac{\left|W_{xy}(f)\right|}{\sqrt{Wxx}(f)\sqrt{Wyy}(f)}$$

Here $x$ and $y$ refer to data from the two regions (i.e., cortical and subcortical). $W_{xy}$ was calculated by taking the sum over time of the complex signal of $x$ multiplied by the conjugate of the complex signal of $y$. $W_{xx}$ and $W_{yy}$ were calculated as the sum over time of the amplitude of each ($x$ and $y$) complex signal. See Figure 2E for an example of coherence at all frequencies in one patient.

Between-region PAC was calculated in the same way as within-region PAC described above, except that the low-frequency phase component and the high-frequency amplitude component were derived from signals from different brain regions (M1 ECoG and subcortical LFP). We examined PAC using both the phase of the subcortical

LFP and amplitude of M1 ECoG and the opposite configuration. See Figure 2F for an example of PAC in one patient.

### Statistical Analysis of Data Grouped across Patients

For statistical comparisons of the change across patients during anesthesia induction, a nonparametric paired sign-rank test was computed comparing, for each patient, the metric of interest (power, within region PAC, coherence, or between region PAC) for data corresponding to the state during which the patient was most awake (State 5, or closest to 5) to the data corresponding to the state during which the patient was most asleep (State 0, or closest to 0). This was done separately for each frequency. Results were then corrected for multiple comparisons (for all frequencies examined) using a false discovery rate (FDR) correction.

## RESULTS

### Propofol and Monitoring Results

Each patient reached an unconscious state (i.e., MOAA/S value = 0 or 1). This was achieved on average in 22.5 min from the start of the file recording (*SD* = 8 min). For each patient, a minimum of three anesthetic states were observed.

### High-frequency Spectral Power Decreases and Low-frequency Power Increases in the Cortex and Subcortical Nuclei

The signal amplitudes were typical for ECoG and LFP data, with an average root mean square value for M1 of 56 μV for the most awake state and 64 μV for the most asleep state ($p < .04$, with a paired, sign-rank test). The subcortical LFP root mean square values were on average 8 μV (not significantly different for awake vs. asleep, $p > .15$; Figure 2).

During induction, the subcortical LFP was characterized by an increase in low-frequency power (4–6 Hz, $p < .05$, FDR-corrected) and a decrease in higher-frequency (broadband) activity (all frequencies 20–250 Hz, $p < .05$, FDR-corrected; Figure 3). In the cortex, a similar pattern was observed for the low-frequency power increase (2–6 Hz, $p < .05$, FDR-corrected) and high-frequency decreases (144–250 Hz, but not all frequencies in this range were significant, $p < .05$). However, the decrease in high-frequency power in the cortex was not significant when correcting for multiple comparisons (Figure 4). Although the cortical high-frequency effect was weak, previous ECoG work has shown similar cortical changes in these frequency ranges during propofol induction (Verdonck, Reed, Hall, Gotman, & Plourde, 2014; Breshears et al., 2010). Thus, although our result was not statistically robust, it trends in the direction reported by others.

Of note, M1 beta power did not change with induction of anesthesia. Although subcortical beta power did decrease during induction, this was a nonspecific effect, because all frequencies above 20 Hz were reduced.

### Coherence between Cortex and Subcortical Nuclei Decreases during Induction

Across patients, there was a spectrally specific decrease in coherence in the beta band (18–24 Hz) during propofol-induced loss of consciousness ($p < .05$, FDR-corrected;

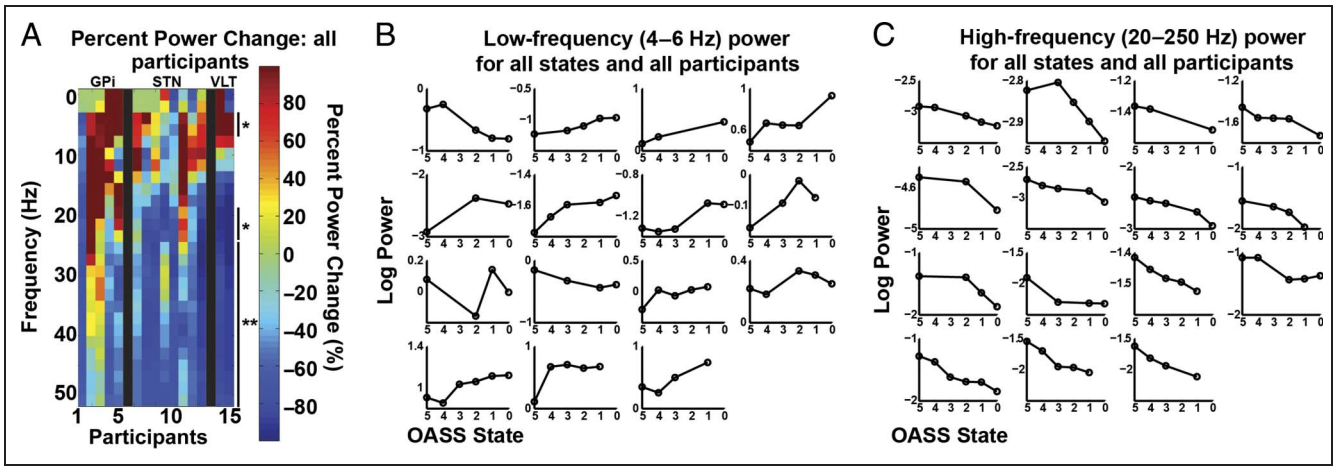


**Figure 3.** Subcortical power changes. (A) Percent power change for all frequencies and participants. Percent change was calculated as: ((asleep − awake) / awake) * 100. Significant differences are indicated with one ($p < .05$, FDR-corrected) or two asterisks ($p < .01$, FDR-corrected). Participants are grouped by region of LFP recordings, indicated with labels (i.e., GPi, STN, and ventrolateral thalamus [VLT]) and separated by black bars. Participant 1 was the dystonia patient, Participants 2–5 and 6–13 were PD patients, and Participants 14–15 were ET patients. To be consistent with subsequent figures, only frequencies below 50 Hz are shown, although higher frequencies were analyzed and described in C. (B) Individual participant log power for each state averaged across the frequencies with a significant increase in power (4–6 Hz). Participant order is the same as in A, with Participants 1–4 making up the first row. (C) Same as B, but showing average log power for all frequencies with a significant decrease during induction (20–250 Hz).

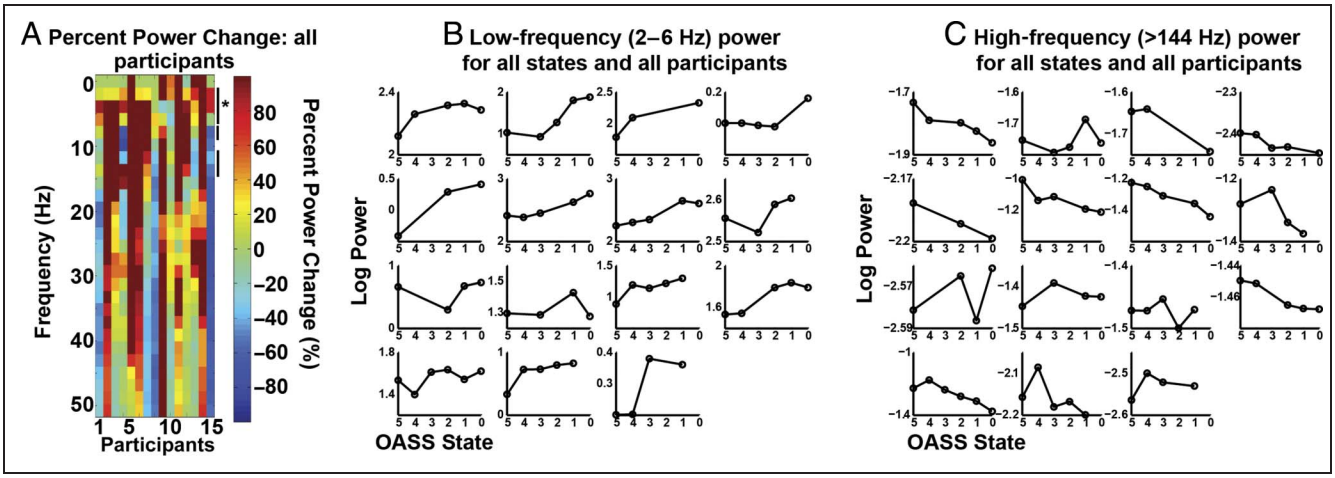


**Figure 4.** M1 power changes. (A) Same as Figure 3A, except M1 power changes. To be consistent with subsequent figures, only frequencies up to 50 Hz are shown, although higher frequencies were analyzed and described in C. The asterisk indicates significant frequencies ($p < .05$, FDR-corrected), and the line without an asterisk indicates significance at $p < .05$, uncorrected. Participants 1, 2, 3, 6, 7, and 8 were recorded with the low-resolution strip. The others were recorded with the high-resolution strip. (B and C) Same as Figure 3B and C except showing M1 power changes for frequencies with a significant increase (B, 2–6 Hz, $p < .05$, FDR-corrected) and (C) significant decrease (>144 Hz, $p < .05$, uncorrected).

Figure 5). This occurred in the setting of no significant change in cortical beta power and a nonspecific decrease in power in all frequencies above 20 Hz in the subcortical LFP. The control analysis for which the same recording durations were used for both the "awake" and "asleep" epochs produced similar results (significant decrease in coherence for 20–24 Hz, $p < .05$ FDR-corrected). Thus, variability in data length is not driving the observed effect.

We also examined the change in the phase of the beta coherence, and although some patients showed a change, it was not consistent across patients (data not shown). Coherence patterns at other frequencies were variable across patients.

## Phase Amplitude Coupling between Cortex and Subcortical Nuclei Decreases during Induction

We calculated PAC in two ways. First, we tested the within-region PAC for M1 and the subcortical target separately and did not observe any significant effects associated with anesthesia induction when correcting for multiple comparisons.

We then calculated inter-region PAC taking the phase from the subcortical target and the amplitude from the M1 ECoG and vice versa. With phase from the subcortical target and amplitude from the M1 ECoG, there was a significant decrease in PAC during induction, again in the beta band (18–20 Hz, $p < .05$, FDR-corrected; see Figure 6). The control analysis for which the same recording durations were analyzed for both the "awake" and "asleep" epochs produced similar, although slightly weaker results (significant decrease in inter-region PAC for 18–20 Hz, $p < .05$, uncorrected). Thus variability in data length is unlikely to be driving the observed effect.

Results in other frequency ranges were variable across participants. Calculating the PAC using the cortical phase and subcortical amplitude revealed no significant results associated with anesthesia induction.

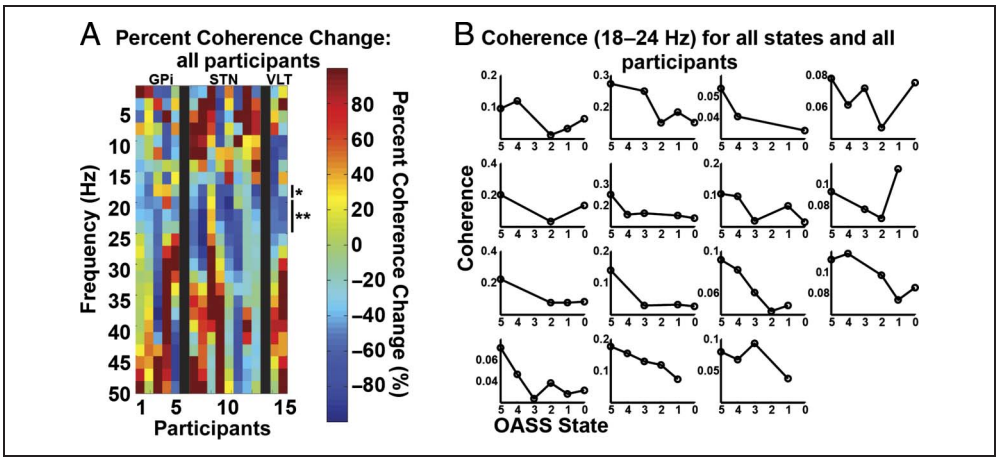


**Figure 5.** M1 and subcortical coherence changes. (A) Same as Figure 3A, except M1 and subcortical coherence changes. Significant differences are indicated with one ($p < .05$, FDR-corrected) or two asterisks ($p < .01$, FDR-corrected). (B) Individual participant coherence shown for each state for 18–24 Hz. Participant order is the same as in Figure 3B.

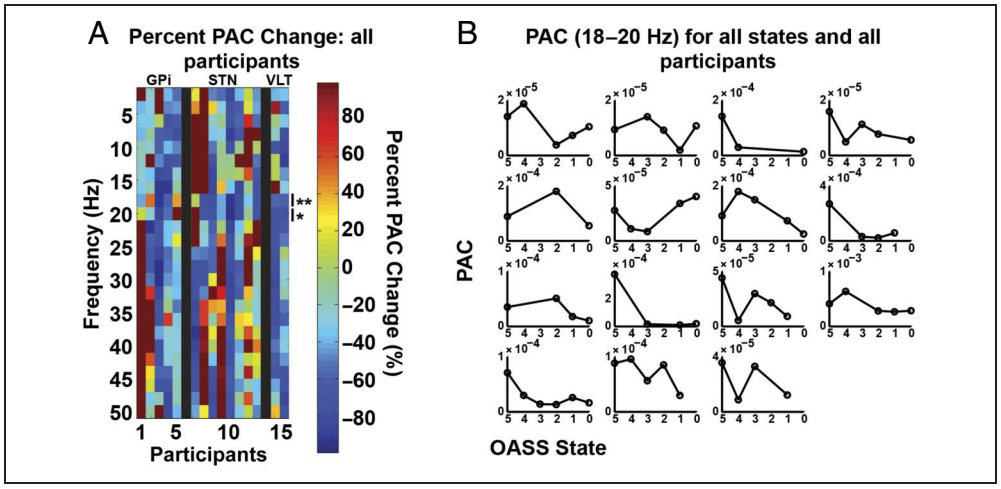


**Figure 6.** M1 and subcortical PAC changes. PAC is calculated using subcortical phase and broadband M1 amplitude (70–150 Hz). (A) Same as Figure 3A, except PAC changes. Significant differences are indicated with one ($p < .05$, FDR-corrected) or two asterisks ($p < .01$, FDR-corrected). (B) Individual participant PAC averaged between 18 and 20 Hz. Participant order is the same as in Figure 3B.

## DISCUSSION

To evaluate changes in interactions between connected brain regions of the motor network associated with loss of consciousness, we collected multisite field potential recordings from structures in the motor network in 15 participants undergoing DBS surgery and examined changes in oscillatory activity. We found a decrease in interactions, measured with coherence and inter-region PAC, between brain regions in BGTC loops during loss of consciousness, specific to the beta band. Importantly, the beta frequency band was the only band to have a consistent change in between-structure coherence and PAC across participants, and this was not the case for cortical or subcortical spectral power. We also observed a decrease in broadband gamma activity in the subcortical nuclei and a similar, although weaker, decrease in cortex. This was accompanied by an increase in low-frequency power in both cortex and subcortical nuclei.

Throughout the brain, cortical structures communicate with functionally homologous subcortical modulators, and this communication is thought to be mediated in part by synchronization in oscillatory activity. The motor system represents one such pair, with well-characterized anatomic connections from cortical motor areas to basal ganglia and thalamus (Alexander et al., 1986), and robust oscillatory activity that is predominant in the alpha or beta range (van Wijk, Beek, & Daffertshofer, 2012; Crone, Miglioretti, Gordon, Sieracki, et al., 1998; Pfurtscheller, 1981). Our focus on the motor system was motivated by the fact that it can be ethically studied using invasive electrophysiological methods during DBS surgery. We expect that the motor system is a reasonable model for other brain networks and that some of the observed patterns may be generally applicable, with network-dependent variation in the particular frequency that is most strongly influenced. Changes in coherence and PAC, reflecting interactions between brain regions, have been shown to vary with changes in behavior in a number of different brain networks (Siegel et al., 2012; Canolty & Knight, 2010). Furthermore, some of the cortical patterns we observe in the motor system are similar to those observed in another ECoG study, which examined more widespread regions of cortex (Breshears et al., 2010). However, because we focused specifically on the motor system, we cannot be sure of the generalizability of our results.

### Support for the Importance of Synchronized Beta Activity in the Motor System

Converging evidence suggests that one consequence of loss of consciousness is functional disconnection between distributed brain regions (Sarasso et al., 2014; Lewis et al., 2012; Alkire et al., 2008; Laureys, 2005; Engel & Singer, 2001). For cortical and subcortical interactions, in particular, this hypothesis is supported by functional imaging studies of the recovery of awareness following traumatic unconsciousness (Laureys & Schiff, 2012; Goldfine & Schiff, 2011) and by the finding that cortical–subcortical structural connectivity correlates with levels of awareness in patients with severe head trauma (Zheng, Reggente, Lutkenhoff, Owen, & Monti, 2014; Fernandez-Espejo et al., 2011). Our results support this hypothesis because two measures that reflect interactions between brain regions, coherence and cross-structure PAC, both decrease during loss of consciousness. These measures are not fully independent, because changes in coherence are likely to affect cross-structure PAC.

Communication in different brain networks may occur through synchronization at particular frequencies, with the specific frequency varying, depending on the brain network (Siegel et al., 2012; Fries, 2005). The motor network is dominated by activity in the alpha–beta range (Miller et al., 2012; Yanagisawa et al., 2012; Brovelli et al., 2004; Kuhn et al., 2004; Cassidy et al., 2002; Crone, Miglioretti, Gordon, Sieracki, et al., 1998; Sanes & Donoghue, 1993; Murthy & Fetz, 1992; Pfurtscheller, 1981). Thus, the reduction in beta coherence seen in this study would be

expected to impair communication between the motor cortex and its subcortical modulators, consistent with the "communication through coherence" hypothesis (Fries, 2005). PAC provides a mechanism to explain how coherence might influence local neural activity (Canolty & Knight, 2010; Canolty et al., 2006). Thus, our observed coherence and PAC decreases are consistent with a general reduction in motor network connectivity and, perhaps, communication, which can be detected with both metrics. We predict that a similar phenomenon might be observed in a different frequency range if a different brain network (with a different predominant frequency range) were studied.

### Opposing Patterns of Functional Connectivity in Consciousness

Some studies, similar to our own, show a decrease in synchrony between distributed areas during loss of consciousness (Chennu et al., 2014; Sarasso et al., 2014; Bonhomme, Boveroux, Brichant, Laureys, & Boly, 2012; Massimini, Ferrarelli, Sarasso, & Tononi, 2012; Laureys et al., 1999), whereas others showed an increase (Mukamel et al., 2014; Breshears et al., 2010; Ching, Cimenser, Purdon, Brown, & Kopell, 2010; Arthuis et al., 2009; Feshchenko, Veselis, & Reinsel, 2004). One explanation for these seemingly contradictory findings may lie in the distinction between "healthy" synchrony, necessary to coordinate communication between separated brain areas (Siegel et al., 2012; Fries, 2005), and abnormal oscillatory patterns, which may break up normally synchronized activity or constrain neural activity in an inflexible pattern. Anesthesia may cause some populations of neurons to fire in an oscillatory, inflexible, way, which then precludes patterns of synchronization necessary for conscious behavior. Indeed, there have been studies that observe both patterns during loss of consciousness, that is, both an increase in oscillatory activity in certain frequency ranges or brain networks, coincident with a decrease in oscillatory activity in others (Purdon et al., 2013; Lewis et al., 2012).

### Alternative Interpretations of the Coherence and PAC Results

We have observed a decrease in coherence and PAC during anesthesia induction that is specific to the beta band and not accompanied by a change in beta power in cortex (and only a general decrease in all frequencies >20 Hz in subcortical areas). We interpret this as a reflection of a reduction in communication throughout the motor system, which occurs specifically in beta. However, alternative interpretations are possible. For instance, the power decrease in the subcortical regions may make the subcortical phase estimate of beta less reliable, reducing coherence. We cannot rule out this interpretation, however, if this were the only factor driving the effect, we might expect a more broadband coherence change, because all frequencies above 20 Hz decreased in the subcortical areas. Furthermore, this interpretation is not necessarily mutually exclusive with the hypothesis that communication at specific frequencies is decreased, because a decrease in communication could also be driven by a decrease in power at the dominant frequency for a particular structure within a brain network.

Another interpretation is that movement could have influenced the recordings, because beta is modulated by movement (Crone, Miglioretti, Gordon, Sieracki, et al., 1998; Pfurtscheller, 1981). Although all our patients were at rest during the recordings, perhaps subtle, undetectable movements were present in the early portions of the recording that decreased over time with anesthesia induction. However, this interpretation would predict changes opposite to those observed here (i.e., an increase in coherence with anesthesia induction), because movement has been associated with a decrease in coherence in the alpha/beta range between cortical and subcortical motor structures (Alegre et al., 2010; Lalo et al., 2008; Cassidy et al., 2002).

### Changes in Power in Specific Brain Regions May Reflect Reduced Neuronal Activity or Relate to Disconnection between Brain Regions

The propofol-induced reduction in cortical broadband activity that we observed was weak but is in general agreement with previous human studies examining ECoG during anesthesia induction (Verdonck et al., 2014; Breshears et al., 2010). The subcortical broadband gamma reduction confirms similar findings in rodent studies (Reed, Plourde, Tobin, & Chapman, 2013) and in one small series of thalamic recordings in humans (Verdonck et al., 2014). Broadband gamma power in cortex is thought to be an index of local neural activity and a surrogate for neural spiking (Manning et al., 2009; Miller et al., 2007). The interpretation of broadband gamma in subcortical structures is less clear but may similarly represent the sum of local neuronal spiking. Indeed, event-related broadband gamma changes similar to those reported in cortex have been observed in subcortical structures (Hamame, Alario, Llorens, Liegeois-Chauvel, & Trebuchon-Da Fonseca, 2014; Ray et al., 2012).

Gamma power decreases are often associated with low-frequency power increases (Crone, Miglioretti, Gordon, & Lesser, 1998; Crone, Miglioretti, Gordon, Sieracki, et al., 1998). The low-frequency power increases (2–6 Hz) that we observe in both cortex and subcortex may relate to this same process. Therefore, one interpretation is that the changes in power observed during loss of consciousness relate to decreased neural activity in regions that play key roles in generating behavior.

An alternative explanation is that the low-frequency (2–6 Hz) power changes in both cortex and subcortex have a different etiology than the high-frequency power changes. Several studies have reported low-frequency power

increases in cortex during anesthesia induction (Verdonck et al., 2014; Purdon et al., 2013; Lewis et al., 2012; Breshears et al., 2010). In some cases, this emerging low-frequency activity is asynchronous across cortex and has been interpreted as a mechanism whereby different brain networks become disconnected from one another (Purdon et al., 2013; Lewis et al., 2012). In many of these studies, the low-frequency activity is in a slightly lower-frequency range (<2 Hz) than is observed here; nevertheless, other studies have shown these changes over a broader frequency range (Verdonck et al., 2014), and so it is possible that a similar mechanism is involved.

### Limitations

There are several limitations to our study. Although our recording methods have high temporal resolution, the precision with which the state of consciousness is assessed, using standard anesthesia scales, is less temporally precise. This may have limited the changes we could detect. All our participants were movement disorder patients who necessarily have abnormal motor networks, and subcortical recording sites were limited to clinically indicated targets for ethical reasons. We sought to minimize this problem by including patients with different diagnoses, which presumably have different pathophysiologies, and by focusing on patterns that were consistent across patients. Nevertheless, an alternative interpretation is that activity changes associated with induction reflect the cessation of symptoms, which occurs with anesthesia. Additionally, the inclusion of different diagnoses further increased the heterogeneity of our sample, which may have decreased our sensitivity for finding effects and makes interpretation more complex. Likewise, although examination of multiple subcortical targets allowed us to focus on motifs common to multiple nodes of the BGTC motor loop, it also increased the potential for signal variability. Thus, we may be insensitive to changes that are present most strongly in only certain subcortical regions. Finally, the use of ECoG strip arrays that can be inserted via a burr hole limited our spatial sampling. Our results may not generalize to the entire cortex (although there are similarities between our data and that recorded with a greater spatial sampling; see Breshears et al., 2010). Investigation of other, more distributed brain networks was precluded by the ethical constraints of working with human patients in the operating room.

### Conclusion

Using a method that allowed us to simultaneously collect high spatial and temporal resolution data from human cortex and subcortical nuclei, we have shown a narrowband reduction in motor system interactions in the beta band across participants during loss of consciousness. These results support a mechanism for communication throughout brain networks that involves synchronous oscillatory activity that is frequency-specific and breaks down when organized recruitment of a brain network for behavior is impossible (i.e., during unconsciousness). These results shed light on possible general mechanisms of neural communication in the human brain.


### Acknowledgments

We would like to thank Dr. Jill Ostrem for help with patient recruitment, Dr. Oana Maties for help with anesthesia assessments, and Dr. Bradley Voytek for helpful comments on the manuscript. We would also like to thank all the patients who participated in this study. This work was supported by the National Institutes of Health (grant R01NS069779 to P. A. S.).



Reprint requests should be sent to Nicole C. Swann, Health Sciences East, Rm #823, 513 Parnassus Avenue, San Francisco, CA 94143, or via e-mail: Nicole.Swann@ucsf.edu.




## REFERENCES


Alegre, M., Rodriguez-Oroz, M. C., Valencia, M., Perez-Alcazar, M., Guridi, J., Iriarte, J., et al. (2010). Changes in subthalamic activity during movement observation in Parkinson's disease: Is the mirror system mirrored in the basal ganglia? *Clinical Neurophysiology, 121,* 414–425.

Alexander, G. E., DeLong, M. R., & Strick, P. L. (1986). Parallel organization of functionally segregated circuits linking basal ganglia and cortex. *Annual Review of Neuroscience, 9,* 357–381.

Alkire, M. T., Hudetz, A. G., & Tononi, G. (2008). Consciousness and anesthesia. *Science, 322,* 876–880.

Arthuis, M., Valton, L., Regis, J., Chauvel, P., Wendling, F., Naccache, L., et al. (2009). Impaired consciousness during temporal lobe seizures is related to increased long-distance cortical-subcortical synchronization. *Brain, 132,* 2091–2101.

Bonhomme, V., Boveroux, P., Brichant, J. F., Laureys, S., & Boly, M. (2012). Neural correlates of consciousness during general anesthesia using functional magnetic resonance imaging (fMRI). *Archives Italiennes de Biologie, 150,* 155–163.

Breshears, J. D., Roland, J. L., Sharma, M., Gaona, C. M., Freudenburg, Z. V., Tempelhoff, R., et al. (2010). Stable and dynamic cortical electrophysiology of induction and emergence with propofol anesthesia. *Proceedings of the National Academy of Sciences, U.S.A., 107,* 21170–21175.

Brovelli, A., Ding, M., Ledberg, A., Chen, Y., Nakamura, R., & Bressler, S. L. (2004). Beta oscillations in a large-scale sensorimotor cortical network: Directional influences revealed by Granger causality. *Proceedings of the National Academy of Sciences, U.S.A., 101,* 9849–9854.

Canolty, R. T., Edwards, E., Dalal, S. S., Soltani, M., Nagarajan, S. S., Kirsch, H. E., et al. (2006). High gamma power is phase-locked to theta oscillations in human neocortex. *Science, 313,* 1626–1628.

Canolty, R. T., & Knight, R. T. (2010). The functional role of cross-frequency coupling. *Trends in Cognitive Sciences, 14,* 506–515.

Cassidy, M., Mazzone, P., Oliviero, A., Insola, A., Tonali, P., Di Lazzaro, V., et al. (2002). Movement-related changes in synchronization in the human basal ganglia. *Brain, 125,* 1235–1246.

Chennu, S., Finoia, P., Kamau, E., Allanson, J., Williams, G. B., Monti, M. M., et al. (2014). Spectral signatures of reorganised brain networks in disorders of consciousness. *PLoS Computational Biology, 10,* e1003887.

Chernik, D. A., Gillings, D., Laine, H., Hendler, J., Silver, J. M., Davidson, A. B., et al. (1990). Validity and reliability of the Observer's Assessment of Alertness/Sedation Scale: Study with intravenous midazolam. *Journal of Clinical Psychopharmacology, 10,* 244–251.

Ching, S., Cimenser, A., Purdon, P. L., Brown, E. N., & Kopell, N. J. (2010). Thalamocortical model for a propofol-induced alpha-rhythm associated with loss of consciousness. *Proceedings of the National Academy of Sciences, U.S.A., 107,* 22665–22670.

Crone, N. E., Miglioretti, D. L., Gordon, B., & Lesser, R. P. (1998). Functional mapping of human sensorimotor cortex with electrocorticographic spectral analysis. II. Event-related synchronization in the gamma band. *Brain, 121,* 2301–2315.

Crone, N. E., Miglioretti, D. L., Gordon, B., Sieracki, J. M., Wilson, M. T., Uematsu, S., et al. (1998). Functional mapping of human sensorimotor cortex with electrocorticographic spectral analysis. I. Alpha and beta event-related desynchronization. *Brain, 121,* 2271–2299.

Crowell, A. L., Ryapolova-Webb, E. S., Ostrem, J. L., Galifianakis, N. B., Shimamoto, S., Lim, D. A., et al. (2012). Oscillations in sensorimotor cortex in movement disorders: An electrocorticography study. *Brain, 135,* 615–630.

de Hemptinne, C., Ryapolova-Webb, E. S., Air, E. L., Garcia, P. A., Miller, K. J., Ojemann, J. G., et al. (2013). Exaggerated phase-amplitude coupling in the primary motor cortex in Parkinson disease. *Proceedings of the National Academy of Sciences, U.S.A., 110,* 4780–4785.

de Hemptinne, C., Swann, N. C., Ostrem, J. L., Ryapolova-Webb, E. S., San Luciano, M., Galifianakis, N. B., et al. (2015). Therapeutic deep brain stimulation reduces cortical phase amplitude coupling in Parkinson's disease. *Nature Neuroscience, 18,* 779–786.

Delorme, A., & Makeig, S. (2004). EEGLAB: An open source toolbox for analysis of single-trial EEG dynamics including independent component analysis. *Journal of Neuroscience Methods, 134,* 9–21.

Engel, A. K., & Singer, W. (2001). Temporal binding and the neural correlates of sensory awareness. *Trends in Cognitive Sciences, 5,* 16–25.

Fechner, J., Ihmsen, H., Hatterscheid, D., Jeleazcov, C., Schiessl, C., Vornov, J. J., et al. (2004). Comparative pharmacokinetics and pharmacodynamics of the new propofol prodrug GPI 15715 and propofol emulsion. *Anesthesiology, 101,* 626–639.

Fernandez-Espejo, D., Bekinschtein, T., Monti, M. M., Pickard, J. D., Junque, C., Coleman, M. R., et al. (2011). Diffusion weighted imaging distinguishes the vegetative state from the minimally conscious state. *Neuroimage, 54,* 103–112.

Feshchenko, V. A., Veselis, R. A., & Reinsel, R. A. (2004). Propofol-induced alpha rhythm. *Neuropsychobiology, 50,* 257–266.

Follett, K. A., Weaver, F. M., Stern, M., Hur, K., Harris, C. L., Luo, P., et al. (2010). Pallidal versus subthalamic deep-brain stimulation for Parkinson's disease. *New England Journal of Medicine, 362,* 2077–2091.

Fries, P. (2005). A mechanism for cognitive dynamics: Neuronal communication through neuronal coherence. *Trends in Cognitive Sciences, 9,* 474–480.

Goldfine, A. M., & Schiff, N. D. (2011). Consciousness: Its neurobiology and the major classes of impairment. *Neurologic Clinics, 29,* 723–737.

Hamame, C. M., Alario, F. X., Llorens, A., Liegeois-Chauvel, C., & Trebuchon-Da Fonseca, A. (2014). High frequency gamma activity in the left hippocampus predicts visual object naming performance. *Brain and Language, 135,* 104–114.

Kuhn, A. A., Williams, D., Kupsch, A., Limousin, P., Hariz, M., Schneider, G. H., et al. (2004). Event-related beta desynchronization in human subthalamic nucleus correlates with motor performance. *Brain, 127,* 735–746.

Lalo, E., Thobois, S., Sharott, A., Polo, G., Mertens, P., Pogosyan, A., et al. (2008). Patterns of bidirectional communication between cortex and basal ganglia during movement in patients with Parkinson disease. *Journal of Neuroscience, 28,* 3008–3016.

Laureys, S. (2005). The neural correlate of (un)awareness: Lessons from the vegetative state. *Trends in Cognitive Sciences, 9,* 556–559.

Laureys, S., Goldman, S., Phillips, C., Van Bogaert, P., Aerts, J., Luxen, A., et al. (1999). Impaired effective cortical connectivity in vegetative state: Preliminary investigation using PET. *Neuroimage, 9,* 377–382.

Laureys, S., & Schiff, N. D. (2012). Coma and consciousness: Paradigms (re)framed by neuroimaging. *Neuroimage, 61,* 478–491.

Lewis, L. D., Weiner, V. S., Mukamel, E. A., Donoghue, J. A., Eskandar, E. N., Madsen, J. R., et al. (2012). Rapid fragmentation of neuronal networks at the onset of propofol-induced unconsciousness. *Proceedings of the National Academy of Sciences, U.S.A., 109,* E3377–E3386.

Manning, J. R., Jacobs, J., Fried, I., & Kahana, M. J. (2009). Broadband shifts in local field potential power spectra are correlated with single-neuron spiking in humans. *Journal of Neuroscience, 29,* 13613–13620.

Massimini, M., Ferrarelli, F., Sarasso, S., & Tononi, G. (2012). Cortical mechanisms of loss of consciousness: Insight from TMS/EEG studies. *Archives Italiennes de Biologie, 150,* 44–55.

Miller, K. J., Hermes, D., Honey, C. J., Hebb, A. O., Ramsey, N. F., Knight, R. T., et al. (2012). Human motor cortical activity is selectively phase-entrained on underlying rhythms. *PLoS Computational Biology, 8,* e1002655.

Miller, K. J., Leuthardt, E. C., Schalk, G., Rao, R. P. N., Anderson, N. R., Moran, D. W., et al. (2007). Spectral changes in cortical surface potentials during motor movement. *Journal of Neuroscience, 27,* 2424–2432.

Mukamel, E. A., Pirondini, E., Babadi, B., Wong, K. F., Pierce, E. T., Harrell, P. G., et al. (2014). A transition in brain state during propofol-induced unconsciousness. *Journal of Neuroscience, 34,* 839–845.

Murthy, V. N., & Fetz, E. E. (1992). Coherent 25- to 35-Hz oscillations in the sensorimotor cortex of awake behaving monkeys. *Proceedings of the National Academy of Sciences, U.S.A., 89,* 5670–5674.

Papavassiliou, E., Rau, G., Heath, S., Abosch, A., Barbaro, N. M., Larson, P. S., et al. (2004). Thalamic deep brain stimulation for essential tremor: Relation of lead location to outcome. *Neurosurgery, 54,* 1120–1129; discussion 1129–1130.

Pfurtscheller, G. (1981). Central beta rhythm during sensorimotor activities in man. *Electroencephalography and Clinical Neurophysiology, 51,* 253–264.

Purdon, P. L., Pierce, E. T., Mukamel, E. A., Prerau, M. J., Walsh, J. L., Wong, K. F., et al. (2013). Electroencephalogram signatures of loss and recovery of consciousness from propofol. *Proceedings of the National Academy of Sciences, U.S.A., 110,* E1142–E1151.

Ray, N. J., Brittain, J. S., Holland, P., Joundi, R. A., Stein, J. F., Aziz, T. Z., et al. (2012). The role of the subthalamic nucleus in response inhibition: Evidence from local field potential recordings in the human subthalamic nucleus. *Neuroimage, 60,* 271–278.

Raz, A., Eimerl, D., Zaidel, A., Bergman, H., & Israel, Z. (2010). Propofol decreases neuronal population spiking activity in the subthalamic nucleus of Parkinsonian patients. *Anesthesia and Analgesia, 111,* 1285–1289.

Reed, S. J., Plourde, G., Tobin, S., & Chapman, C. A. (2013). Partial antagonism of propofol anaesthesia by physostigmine in rats is associated with potentiation of fast (80–200 Hz) oscillations in the thalamus. *British Journal of Anaesthesia, 110,* 646–653.

Sanes, J. N., & Donoghue, J. P. (1993). Oscillations in local field potentials of the primate motor cortex during voluntary movement. *Proceedings of the National Academy of Sciences, U.S.A., 90,* 4470–4474.

Sarasso, S., Rosanova, M., Casali, A. G., Casarotto, S., Fecchio, M., Boly, M., et al. (2014). Quantifying cortical EEG responses to TMS in (un)consciousness. *Clinical EEG and Neuroscience, 45,* 40–49.

Shahlaie, K., Larson, P. S., & Starr, P. A. (2011). Intraoperative computed tomography for deep brain stimulation surgery: Technique and accuracy assessment. *Neurosurgery, 68,* 114–124; discussion 124.

Shimamoto, S. A., Ryapolova-Webb, E. S., Ostrem, J. L., Galifianakis, N. B., Miller, K. J., & Starr, P. A. (2013). Subthalamic nucleus neurons are synchronized to primary motor cortex local field potentials in Parkinson's disease. *Journal of Neuroscience, 33,* 7220–7233.

Siegel, M., Donner, T. H., & Engel, A. K. (2012). Spectral fingerprints of large-scale neuronal interactions. *Nature Reviews Neuroscience, 13,* 121–134.

Smith, C., McEwan, A. I., Jhaveri, R., Wilkinson, M., Goodman, D., Smith, L. R., et al. (1994). The interaction of fentanyl on the Cp50 of propofol for loss of consciousness and skin incision. *Anesthesiology, 81,* 820–828; discussion 826A.

Starr, P. A., Christine, C. W., Theodosopoulos, P. V., Lindsey, N., Byrd, D., Mosley, A., et al. (2002). Implantation of deep brain stimulators into the subthalamic nucleus: Technical approach and magnetic resonance imaging-verified lead locations. *Journal of Neurosurgery, 97,* 370–387.

Starr, P. A., Turner, R. S., Rau, G., Lindsey, N., Heath, S., Volz, M., et al. (2006). Microelectrode-guided implantation of deep brain stimulators into the globus pallidus internus for dystonia: Techniques, electrode locations, and outcomes. *Journal of Neurosurgery, 104,* 488–501.

Tort, A. B., Kramer, M. A., Thorn, C., Gibson, D. J., Kubota, Y., Graybiel, A. M., et al. (2008). Dynamic cross-frequency couplings of local field potential oscillations in rat striatum and hippocampus during performance of a T-maze task. *Proceedings of the National Academy of Sciences, U.S.A., 105,* 20517–20522.

van Wijk, B. C., Beek, P. J., & Daffertshofer, A. (2012). Neural synchrony within the motor system: What have we learned so far? *Frontiers in Human Neuroscience, 6,* 252.

Verdonck, O., Reed, S. J., Hall, J., Gotman, J., & Plourde, G. (2014). The sensory thalamus and cerebral motor cortex are affected concurrently during induction of anesthesia with propofol: A case series with intracranial electroencephalogram recordings. *Canadian Journal of Anaesthesia, 61,* 254–262.

Yanagisawa, T., Yamashita, O., Hirata, M., Kishima, H., Saitoh, Y., Goto, T., et al. (2012). Regulation of motor representation by phase-amplitude coupling in the sensorimotor cortex. *Journal of Neuroscience, 32,* 15467–15475.

Yousry, T. A., Schmid, U. D., Alkadhi, H., Schmidt, D., Peraud, A., Buettner, A., et al. (1997). Localization of the motor hand area to a knob on the precentral gyrus. A new landmark. *Brain, 120,* 141–157.

Zheng, Z., Reggente, N., Lutkenhoff, E., Owen, A. M., & Monti, M. (2014). Structural connectivity between the thalamus and fronto-temporal regions predicts level of awareness in disorders of consciousness. *Society for Neuroscience Conference (Abs)*.